Secondary Ion MS Imaging of Lipids in Picoliter Vials with a Buckminsterfullerene Ion Source

ARTICLE *in* ANALYTICAL CHEMISTRY · NOVEMBER 2005

Impact Factor: 5.64 · DOI: 10.1021/ac0508189 · Source: PubMed

7 AUTHORS, INCLUDING:

Thomas P Roddy
Merck
66 PUBLICATIONS **1,114** CITATIONS
SEE PROFILE

Andrew G Ewing
University of Gothenburg
191 PUBLICATIONS **5,297** CITATIONS
SEE PROFILE

Anal. Chem. **2005,** *77,* 6190−6196

Secondary Ion MS Imaging of Lipids in Picoliter Vials with a Buckminsterfullerene Ion Source

Sara G. Ostrowski, Christopher Szakal, Joseph Kozole, Thomas P. Roddy, Jiyun Xu, Andrew G. Ewing, and Nicholas Winograd*

Department of Chemistry, 104 Chemistry Research Building, Pennsylvania State University, University Park, Pennsylvania 16802

Investigation of the spatial distribution of lipids in cell membranes can lead to an improved understanding of the role of lipids in biological function and disease. Time-of-flight secondary ion mass spectrometry is capable of molecule-specific imaging of biological molecules across single cells and has demonstrated potential for examining the functional segregation of lipids in cell membranes. In this paper, standard SIMS spectra are analyzed for phosphatidylethanolamine, phosphatidylglycerol, phosphatidylserine, phosphatidylinositol, cholesterol, and sulfatide. Importantly, each of the lipids result in signature mass spectral peaks that allow them to be identified. These signature peaks are also useful for imaging experiments and are utilized here to simultaneously image lipids on a micrometer scale in picoliter vials. Because the low secondary ion signal achieved for lipids from an atomic primary ion source makes cell-imaging experiments challenging, improving signal with cluster primary ion sources is of interest. Here, we compare the secondary ion yield for seven lipids using atomic (Ga^+ or In^+) ion sources and a buckminsterfullerene (C_{60}^+) primary ion source. A 40−1000-fold improvement in signal is found with C_{60}^+ relative to the other two ion sources, indicating great promise for future cellular imaging applications using the C_{60}^+ probe.

Numerous biological functions, including signal transduction, protein regulation, and secretion, are managed by the diverse array of molecules in the cell membrane. Investigation of the subtle intricacies of membrane proteins and lipids is essential to gaining an improved knowledge of cellular events. Although a certain amount of lateral fluidity exists among the membrane lipids,[1] domains of restricted lipid diffusion have been observed in cells and model systems.[2−8] A heterogeneous distribution of lipids may mediate biological function by controlling the curvature of the cell membrane and the interaction of membrane proteins.[9,10] A major limitation in the study of these lipids is the lack of a methodology with high sensitivity and spatial resolution for the lipids.

To elucidate the role of lipid heterogeneity, domains have been studied with a variety of analytical techniques. Experiments with fluorescence techniques[3,6,11] have contributed a great wealth of knowledge about lipid domains, but the techniques suffer from indirect chemical localization, and the fluorescent tags have been shown to interfere with the native chemical distribution of the membrane.[12] Other analytical techniques, such as atomic force microscopy[7] and electron microscopy,[8] give valuable topographical and morphological information, but no chemical specificity. Spatially resolved chemical images of the lipid distribution in single-cell membranes will expand the current understanding of the role of lipid heterogeneity in biological function and disease.

Time-of-flight secondary ion mass spectrometry (TOF-SIMS) can be used for chemical imaging of lipid domains on cell membranes and has been well-established for bioanalytical applications.[13−25] For example, SIMS has been used to image the distribution of phosphatidylcholine (PC) across tissue,[13] Lang-

* Corresponding author. E-mail: nxw@psu.edu.

(1) Singer, S. J.; Nicolson, G. L. *Science* **1972**, *175*, 720−731.
(2) Edidin, M. *Trends Cell. Biol.* **2001**, *11*, 492−496.
(3) Hao, M. M.; Mukherjee, S.; Maxfield, F. R. *Proc. Natl. Acad. Sci. U.S.A.* **2001**, *98*, 13072−13077.
(4) Brown, D. A. *Proc. Natl. Acad. Sci. U.S.A.* **2001**, *98*, 10517−10518.
(5) Yechiel, E.; Edidin, M. *J. Cell Biol.* **1987**, *105*, 755−760.
(6) Hwang, J.; Gheber, L. A.; Margolis, L.; Edidin, M. *Biophys. J.* **1998**, *74*, 2184−2190.
(7) Gliss, C.; Clausen-Schaumann, H.; Gunther, R.; Odenbach, S.; Randl, O.; Bayerl, T. M. *Biophys. J.* **1998**, *74*, 2443−2450.
(8) Rock, P.; Allietta, M.; Young, W. W.; Thompson, T. E.; Tillack, T. W. *Biochemistry* **1990**, *29*, 8484−8490.
(9) Simons, K.; Ehehalt, R. *J. Clin. Invest.* **2002**, *110*, 597−603.
(10) Gruner, S. M. *Proc. Natl. Acad. Sci. U.S.A.* **1985**, *82*, 3665−3669.
(11) Forstner, M. B.; Martin, D. S.; Navar, A. M.; Kas, J. A. *Langmuir* **2003**, *19*, 4876−4879.
(12) Leonard-Latour, M.; Morelis, R. M.; Coulet, P. R. *Langmuir* **1996**, *12*, 4797−4802.
(13) McMahon, J. M.; Short, R. T.; McCandlish, C. A.; Brenna, J. T.; Todd, P. J. *Rapid Commun. Mass Spectrom.* **1996**, *10*, 335−340.
(14) Todd, P. J.; McMahon, J. M.; Short, R. T.; McCandlish, C. A. *Anal. Chem.* **1997**, *69*, 9, A529−A535.
(15) Cannon, D. M.; Pacholski, M. L.; Winograd, N.; Ewing, A. G. *J. Am. Chem. Soc.* **2000**, *122*, 603−610.
(16) Lorey, D. R.; Morrison, G. H.; Chandra, S. *Anal. Chem.* **2001**, *73*, 3947−3953.
(17) Colliver, T. L.; Brummel, C. L.; Pacholski, M. L.; Swanek, F. D.; Ewing, A. G.; Winograd, N. *Anal. Chem.* **1997**, *69*, 2225−2231.
(18) Roddy, T. P.; Cannon, D. M.; Ostrowski, S. G.; Winograd, N.; Ewing, A. G. *Anal. Chem.* **2002**, *74*, 4020−4026.
(19) Ostrowski, S. G.; Van Bell, C. T.; Winograd, N.; Ewing, A. G. *Science* **2004**, *305*, 71−73.
(20) Monroe, E. B.; Jurchen, J. C.; Lee, J.; Rubakhin, S. S.; Sweedler, J. V. *J. Am. Chem. Soc.* **2005**, *127*, 12152−12153.
(21) McQuaw, C. M.; Sostarecz, A. G.; Zheng, L. L.; Ewing, A. G.; Winograd, N. *Langmuir* **2005**, *21*, 807−813.
(22) Bourdos, N.; Kollmer, F.; Benninghoven, A.; Ross, M.; Sieber, M.; Galla, H. J. *Biophys. J.* **2000**, *79*, 357−369.
(23) Sostarecz, A. G.; McQuaw, C. M.; Ewing, A. G.; Winograd, N. *J. Am. Chem. Soc.* **2004**, *126*, 13882−13883.

10.1021/ac0508189 CCC: $30.25
Published on Web 09/02/2005

muir−Blodgett films,[22−24,26] liposomes,[15] and single cells.[18,19,25] In fact, a heterogeneous distribution of PC and 2-aminoethylphosphonolipid was observed at the junction of mating *Tetrahymena*, suggesting these lipids have a role in membrane fusion.[19] SIMS can also be used to investigate nonlipid membrane components, and Sweedler and co-workers have reported a heterogeneous distribution of vitamin E on *Aplysia californica* neuronal membranes, which implies that vitamin E may be important for neuronal functions.[20]

The use of cluster ion primary sources in SIMS is an important advance in the instrumentation that will aid in examining the low concentrations of specialized cell membrane lipids. These cluster sources, notably SF_5^+, gold cluster ions Au_n^+, and buckminsterfullerene, C_{60}^+, boast a greatly improved secondary ion signal that will be essential for future cell membrane investigations.[27−29] In particular, using C_{60}^+, Vickerman et al. have demonstrated over a 100-fold ion yield enhancement for some organic samples.[29] In this paper, the SIMS spectra of PE, PG, PS, PI, cholesterol, and sulfatide are characterized. Unique mass spectral peaks are identified for each comparing the C_{60}^+ and the Ga^+ ion sources. Using the molecule-specific imaging abilities of static TOF-SIMS, we further demonstrate that the signature peaks enable these lipids to be spatially resolved in picoliter vial arrays. A 40−1000-fold improvement in signal is observed with C_{60} for PE, PG, PS, PI, cholesterol, sulfatide, and PC compared to the Ga^+ ion source. This yield enhancement results in better contrast in SIMS images providing greater promise for future studies of the lipid distribution in single cell membranes.

EXPERIMENTAL SECTION

Thick-Film Sample Preparation. Dipalmitoylphosphatidylethanolamine (DPPE), dipalmitoylphosphatidylglycerol (DPPG), dipalmitoylphosphatidylserine (DPPS), soybean phosphatidylinositol (PI), cholesterol, sulfatide, and dipalmitoylphosphatidylcholine (DPPC) (Avanti Polar Lipids, Alabaster, AL) were dissolved in 9:1 chloroform/methanol at a 1 mg/mL concentration. The lipid solutions were spin-coated onto pirhana-etched silicon wafers (Ted Pella, Redding, CA) for standard analyses and mixture experiments.

Picoliter Vial Array Solution Delivery. The imaging experiments utilized picoliter vial arrays nanofabricated at the Cornell University National Nanofabrication Facility, as described elsewhere.[30] Samples were delivered into the picoliter vials using micropipets made from borosilicate capilliaries (Sutter Instrument Co., Novato, CA; P/N B120-69-10, 1.2-mm o.d., 0.69-mm i.d.) that were pulled to a fine tip using a Sutter Instrument Co. pipet puller. For each lipid solution, a virgin micropipet was backfilled using a microliter syringe (Hamilton, Reno, NV); the syringe was thoroughly washed with chloroform before administering the next solution. The nontapered end of each micropipet was attached to a General Valve Picospritzer (Fairfax, NJ), which controlled the delivery volume by regulating the pressure (3 psi) and pulse length (5 ms) applied to the pipet. The tip of the micropipet was positioned to directly contact the bottom of each picoliter vial with the aid of a micromanipulator stage and a stereomicroscope (Leica Stereozoom5, Bannockburn, IL).

Secondary Ion Mass Spectrometry. Unless otherwise noted, experiments were performed on a Kratos Prism TOF-SIMS spectrometer (Manchester, U.K.) equipped with an indium liquid metal ion source (FEI, Beaverton, OR). The pulsed primary ion source was angled at 45° to the sample and was operated at 15-kV beam energy, with a 500-pA beam current, a 200-nm beam diameter at the surface, and a 50-ns pulse width. Secondary ions were electrostatically directed to the time-of-flight tube by a sample stage biased at ±2.5 kV and by an extraction lens oppositely biased at 4.5 kV. Prior to detection by a microchannel plate assembly (Galileo Co., Sturbridge, MA), the secondary ions were mass-separated in a 4.5-m horizontal reflectron time-of-flight path. Spectra for all thick-film lipid analyses were taken from a sample area of 300 × 300 μm^2 and with 1 million primary ion pulses.

Mass spectrometry images were acquired by rastering the primary ion beam across the sample region and collecting a mass spectrum for each pixel in the image. Using computer software written in-house, a peak of interest was then selected in the total ion mass spectrum. The intensity of this mass was plotted in micrometer-scale pixels to generate an image showing the location of the analyte. The color of the pixels could be converted to red, green, or blue using the TOF-SIMS software to distinguish between different chemical maps. Additional colors were possible by using Spot Advanced imaging software (Diagnostic Instruments, Sterling Heights, MI) to alter the hue of the SIMS images. The color-coded chemical maps were overlaid using either the TOF-SIMS software or the Spot Advanced software.

Additional imaging and ion yield comparison experiments were executed using a BioToF TOF-SIMS spectrometer, which features a C_{60} primary ion source and a gallium primary ion source (Ionoptika Ltd., Southampton, U.K.). The instrument and ion sources have been described in detail elsewhere.[29,31] For the C_{60}^+ picoliter imaging experiments, a 300-μm beam-defining aperture in the gun column was used to create a 30-μm probe size and 0.25 nA of primary ion current. In the ion yield comparison experiments, the C_{60}^+ beam was focused to 50 μm with a 1-mm beam-defining aperture and 1.1 nA of primary ion current; the Ga^+ primary ion beam was focused to approximately 200 nm and 3 nA of primary ion current. The smaller probe size was chosen for imaging experiments to allow finer image resolution, but for the ion yield comparison experiments, image resolution was not as important a factor. For all ion yield comparison experiments, a baseline was determined for each lipid peak by finding a nearby flat region of the spectrum and determining the average signal in this region of the spectrum. This value was subtracted from the intensity in every bin for the peak of interest. The ion yields were then determined by calculating the peak area from the baseline-subtracted intensities and normalizing to the primary ion current in nC. Because the ion yield comparison experiments were

(24) Ross, M.; Steinem, C.; Galla, H. J.; Janshoff, A. *Langmuir* **2001**, *17*, 2437−2445.
(25) Roddy, T. P.; Cannon, D. M.; Meserole, C. A.; Winograd, N.; Ewing, A. G. *Anal. Chem.* **2002**, *74*, 4011−4019.
(26) Sostarecz, A. G.; Cannon, D. M.; McQuaw, C. M.; Sun, S. X.; Ewing, A. G.; Winograd, N. *Langmuir* **2004**, *20*, 4926−4932.
(27) Fuoco, E. R.; Gillen, G.; Wijesundara, M. B. J.; Wallace, W. E.; Hanley, L. *J. Phys. Chem. B* **2001**, *105*, 3950−3956.
(28) Touboul, D.; Halgand, F.; Brunelle, A.; Kersting, R.; Tallarek, E.; Hagenhoff, B.; Laprevote, O. *Anal. Chem.* **2004**, *76*, 1550−1559.
(29) Weibel, D.; Wong, S.; Lockyer, N.; Blenkinsopp, P.; Hill, R.; Vickerman, J. C. *Anal. Chem.* **2003**, *75*, 1754−1764.
(30) Braun, R. M.; Beyder, A.; Xu, J. Y.; Wood, M. C.; Ewing, A. G.; Winograd, N. *Anal. Chem.* **1999**, *71*, 3318−3324.
(31) Braun, R. M.; Blenkinsopp, P.; Mullock, S. J.; Corlett, C.; Willey, K. F.; Vickerman, J. C.; Winograd, N. *Rapid Commun. Mass Spectrom.* **1998**, *12*, 1246−1252.

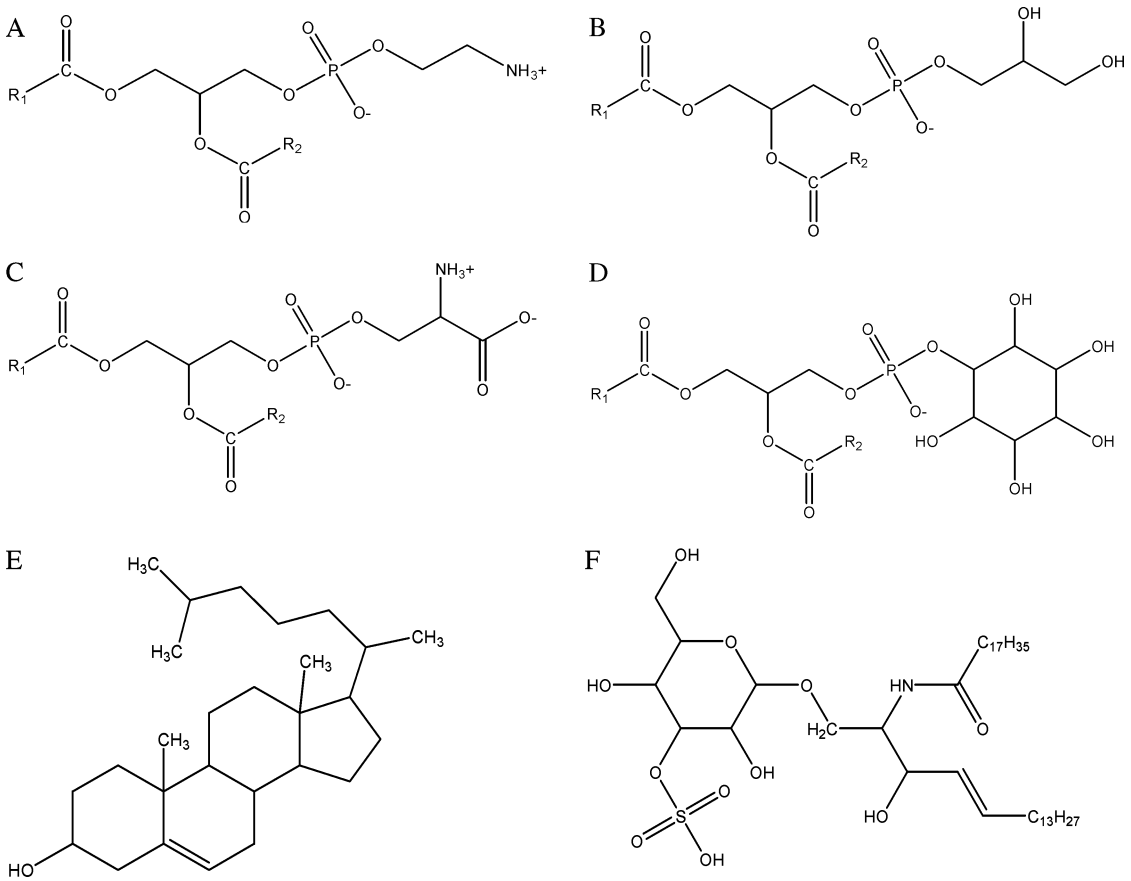

Figure 1. Chemical structures for six lipids. (A) PE, (B) PG, (C) PS, (D) PI (soybean), (E) cholesterol, and (F) sulfatide.

performed on the same samples in the same instrument, parameters that were not associated with differences between the primary ion sources remained constant and it was not necessary to incorporate them into the ion yield calculations. Finally, for all peaks of interest, ratios were taken of the resulting ion yields obtained using the two primary ion sources.

RESULTS AND DISCUSSION

Overview of SIMS of Lipids. The SIMS fragmentation and ionization of PC has been well characterized;[13,32] however, the abundance of diverse and functionally important lipids in the cell membrane necessitates the investigation of the SIMS spectra for other lipids (Figure 1). The nonlamellar phospholipids, phosphatidylethanolamine (PE, Figure 1A), phosphatidylglycerol (PG, Figure 1B), phosphatidylserine (PS, Figure 1C), and phosphatidylinositol (PI, Figure 1D), are interesting membrane species. It is hypothesized that a heterogeneous distribution of nonlamellar lipids drives or restricts membrane fusion events, such as exocytosis, by reducing or increasing the packing constraints associated with highly curved fusion structures.[33] Cholesterol (C, Figure 1E) is also an intriguing lipid because it holds lipid rafts together and because abnormalities in membrane cholesterol levels have been observed in atherosclerosis and bacterial, viral, and pathogenic diseases, such as HIV and Alzheimer disease.[9,34–37] Another notable membrane component is the glycosphingolipid, sulfatide (S, Figure 1F), which is found in many organ tissues. For example, sulfatide is present in the islets of Langerhans in the pancreas, where it is suspected to have a role in insulin trafficking,[38] and is found in myelin, where it may be involved in demyelination diseases, such as multiple sclerosis.[39]

The ionization of six biologically relevant lipids was studied with SIMS in order to provide a basis for future experiments that will assess the involvement of these lipids in cellular events. Standard spectra were generated by analyzing anhydrous films of the individual lipids of interest with an In^+ ion source (Figures 2 and 3). These spectra were compared, and unique positive and negative fragment ion peaks were identified for each of the lipids (Table 1). For the phospholipids, these characteristic peaks were phosphate headgroup fragments because, in general, the samples examined were synthetic dipalmitoyl phospholipids, which all have the same fatty acid side chains. This experimental design was chosen to focus the analysis on the headgroups because the large variety of fatty acid tailgroup structures in a biological membrane makes it difficult to detect molecular ion or subtle tailgroup variations with current SIMS technology. Common positive ion peaks were found at m/z 125 ($C_2H_6PO_4^+$), 143 ($C_8H_{15}O_2^+$), 165,

(32) Roddy, T. P.; Cannon, D. M.; Ostrowski, S. G.; Ewing, A. G.; Winograd, N. *Anal. Chem.* **2003**, *75*, 4087−4094.
(33) Chernomordik, L. *Chem. Phys. Lipids* **1996**, *81*, 203-213.
(34) Lusis, A. J. *Nature* **2000**, *407*, 233−241.
(35) Campbell, S. M.; Crowe, S. M.; Mak, J. *J. Clin. Virol.* **2001**, *22*, 217−227.
(36) Ehehalt, R.; Keller, P.; Haass, C.; Thiele, C.; Simons, K. *J. Cell Biol.* **2003**, *160*, 113−123.
(37) Manie, S. N.; Debreyne, S.; Vincent, S.; Gerlier, D. *J, Virol.* **2000**, *74*, 305−311.
(38) Fredman, P.; Mansson, J. E.; Rynmark, B. M.; Josefsen, K.; Ekblond, A.; Halldner, L.; Osterbye, T.; Horn, T.; Buschard, K. *Glycobiology* **2000**, *10*, 39−50.
(39) Ilyas, A. A.; Chen, Z. W.; Cook, S. D. *J. Neuroimmunol.* **2003**, *139*, 76−80.

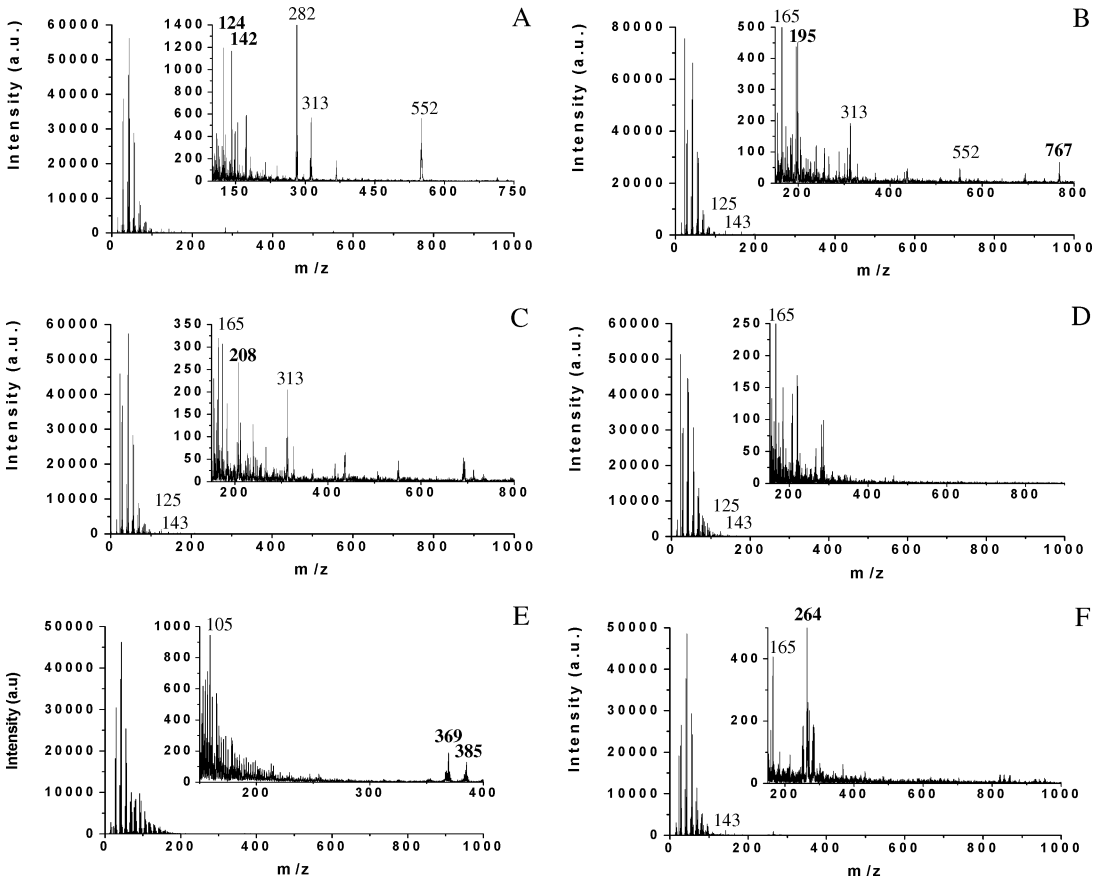

Figure 2. + SIMS spectra for six lipids. (A) DPPE, (B) DPPG, (C) DPPS, (D) PI (soybean), (E) cholesterol, and (F) sulfatide.

313 ($C_{19}H_{37}O_3^+$), and 552 ($C_{35}H_{68}O_4^+$) for most lipids and therefore may be the suggested headgroup fragment peaks, fatty acid fragment peaks, or else contaminants introduced during synthesis or sample preparation. Similarly, common negative ion peaks were *m/z* 79 (PO_3^-), 97 (HPO_4^-), and 137, 153, 181, and 255 ($C_{16}H_{31}O_2^-$, palmitic acid).

Signature peaks were identified for PE, PG, PS, PI, cholesterol, and sulfatide. The ionization of PC has been described in detail.[13,32] Phosphatidylethanolamine ionized to form intense positive ion peaks at *m/z* 142 and 124 corresponding to the phosphate headgroup and the headgroup minus water, respectively, (Figure 2A). The peak observed at *m/z* 282 probably resulted from $C_{18}H_{36}NO^+$, a plastic extrusion lubricant and common laboratory contaminant, and not from PE. The characteristic positive ion peaks for several phospholipids were sodium adducts of the phosphate headgroups (PG, *m/z* 195, (Figure 2B); PS, *m/z* 208 (Figure 2C)); and of the molecular ion (PG, *m/z* 767, (Figure 2B)). These lipids were Na salts, and the formation of matrix adduct ions was expected because there was a high concentration of matrix Na available for ionization and because this ionization behavior has been observed in fast atom bombardment (FAB) MS for phosphatidylserine.[40] Phosphatidylinositol did not exhibit any unique peaks in the positive mode (Figure 2D). For the cholesterol sample, the molecular ion, $(M - H)^+$, was detected at *m/z* 385 and an additional intense positive fragment at *m/z* 369 was identified to be the molecular ion minus a hydroxyl group (Figure 2E). Similar to the Na salts of PG and PS, the characteristic positive ion peak for the sulfatide salt was a Na adduct of the sulfate headgroup minus water (Figure 2F). Because cells are prepared for SIMS analysis in Na-rich buffer solution or cell media, it is possible that the Na adduct ions of lipids would be observed in cell samples. Lipids in cell membranes that are preserved by freeze−fracture sample preparation may preferentially form protonated headgroup ions along with the Na adducts because of the large availability of protons in the water matrix.[32]

The negative ion peaks for PE were detected at *m/z* 122 and 140, which were analogous to the headgroup and headgroup minus water peaks observed in the positive mode (Figure 3A). Ionization of PG also resulted in a unique negative fragment ion at *m/z* 171, which was the deprotonated phosphate headgroup (Figure 3B). The negative ion spectrum of PS did not show any characteristic peaks unique to this lipid (Figure 3C). Phosphatidylinositol exhibited unique fragment peaks only in the negative ion mode of operation at *m/z* 241, 259, and 299, consistent with reports in the literature for FAB-MS (Figure 3D).[40] Cholesterol (Figure 3E) and sulfatide (Figure 3F) spectra indicated a few unique negative ion peaks, which have not yet been identified and may result from contaminants (C, *m/z* 123, 195, 465, 499) (S, *m/z* 217, 261). The positive and negative ion signature peaks should be unique to these lipids found in complex biological systems. Proteins typically fragment during the SIMS process to form low-mass peaks (below *m/z* 100) and should not cause isobaric interferences with the lipids of interest.[41]

Chemical Imaging in Picoliter Vials. To determine whether the signature peaks discussed in this paper could be used to chemically map the lipids in spatially different environments, an

(40) Murphy, R. C. *Mass Spectrometry of Lipids*; Plenum Press: New York, 1993.

(41) Wagner, M. S.; Castner, D. G. *Langmuir* **2001**, *17*, 4649−4660.

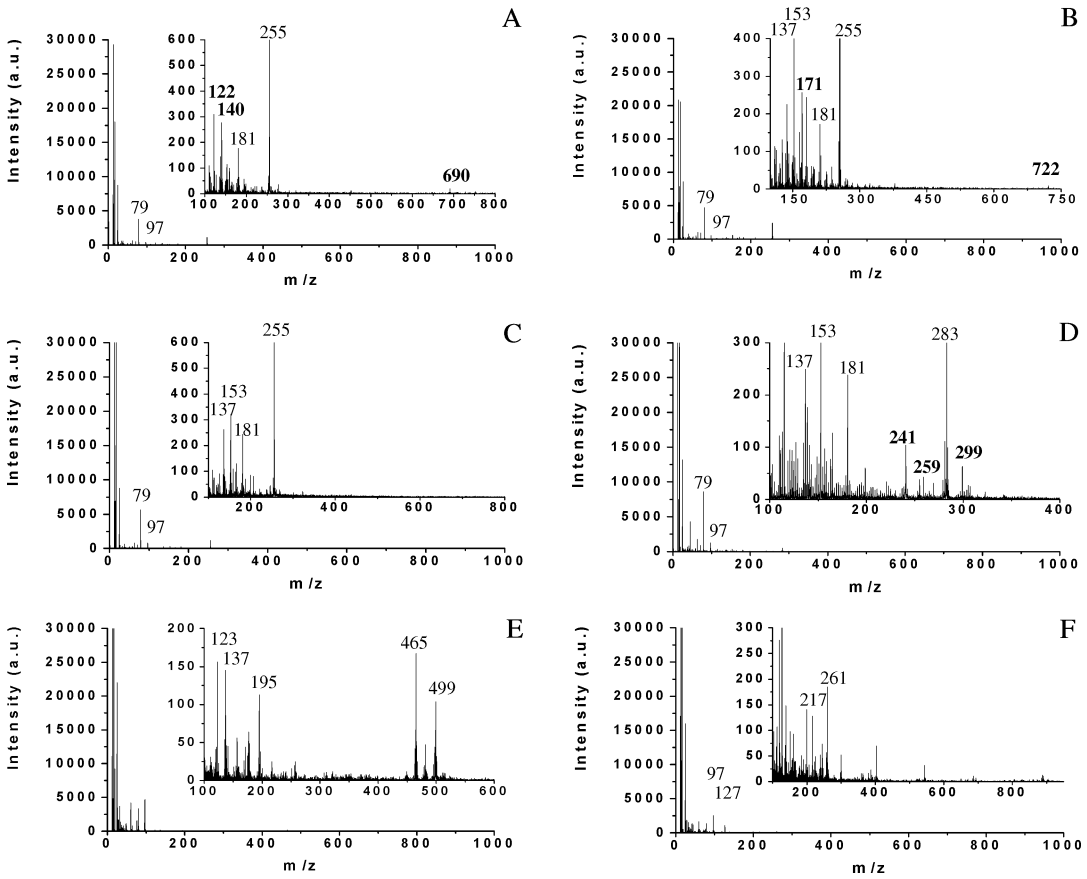

Figure 3. −SIMS spectra for six lipids. (A) DPPE, (B) DPPG, (C) DPPS, (D) PI (soybean), (E) cholesterol, and (F) sulfatide.

Table 1. Characteristic SIMS Fragment Peaks for Various Lipid Classes

lipid	fragment	calculated mass (m/z)
phosphatidylcholine	$C_5H_{12}N^+$	86.0970
phosphatidylcholine	$C_5H_{15}NPO_4^+$	184.0739
phosphatidylcholine	$C_8H_{19}NPO_4^+$	224.1052
phosphatidylethanolamine	$C_2H_7NPO_3^+$	124.0164
phosphatidylethanolamine	$C_2H_9NPO_4^+$	142.0269
phosphatidylethanolamine	$C_2H_5NPO_3^-$	122.0007
phosphatidylethanolamine	$C_2H_7NPO_4^-$	140.0113
phosphatidylglycerol	$C_3H_9PO_6Na^+$	195.0035
phosphatidylglycerol	$C_3H_9PO_6^-$	171.0059
phosphatidylinositol	$C_6H_{10}PO_8^-$	241.0114
phosphatidylinositol	$C_6H_{12}PO_9^-$	259.0219
phosphatidylinositol	$C_9H_{16}PO_9^-$	299.0533
phosphatidylserine	$C_3H_8NPO_6Na^+$	207.9988
cholesterol	$C_{27}H_{45}^+$	369.3521
cholesterol	$C_{27}H_{45}O^+$	385.3470
sulfatide	$C_6H_9SO_8Na^+$	263.9916

array of lithographically fabricated picoliter vials was used. Four different lipids were delivered one by one into adjacent silicon picoliter vials (Figure 4). The imaging area of the instrument has a maximum field of view of 400 × 400 μm, which is slightly larger than four vials. Figure 4A shows an image of the four lipids in picoliter vials obtained with an In^+ ion source. Signals from PC (m/z 184), PG (m/z 195), and sulfatide (m/z 264) headgroups and from cholesterol (m/z 369) were localized to the vials into which they were delivered. In this image, the blue pixels represent regions of high silicon signal and black pixels represent low silicon signal due to substrate coverage by the lipid film. The void in signal also indicates that the lipid signal is quite low under these experimental conditions, emphasizing the importance of improving secondary ion yield for biological species.

Use of the C_{60}^+ Ion Source for Lipids. One method of increasing the signal of large organic species, such as the lipids in question, is to increase the sputter yield by using cluster ion primary sources, like C_{60}^+. Molecular dynamic simulations suggest that, in contrast to atomic projectiles such as In^+ and Ga^+, C_{60}^+ cluster projectiles break into and disperse the primary projectile energy among individual carbon atoms upon surface impact.[42] This phenomenon allows for a more shallow penetration depth and more surface-localized primary bombardment energy for cluster projectiles in comparison to their atomic counterparts. An additional benefit is that large, intact molecules are gently lifted off the surface by this "softer" C_{60}^+ sputtering process.[42] Therefore, C_{60}^+ and other cluster ion sources are attractive alternatives as SIMS primary ion sources for biological applications, where there is a desire to greatly reduce molecular fragmentation of larger-mass target analytes. To evaluate the magnitude of signal improvement for lipids with C_{60}^+, the picoliter vial array was also imaged in a separate SIMS instrument equipped with the cluster ion source (Figure 4B). Clearly, the C_{60}^+ bombardment resulted in a dramatic increase in signal from the lipids. Interestingly, while the positive ion lipid signals using C_{60}^+ were increased between 80- and 700-fold compared to the yield when In^+ was used, the signal from nearby silicon was changed by only 4-fold. This result is not surprising because the real advantage of the C_{60}^+ source

(42) Postawa, Z.; Czerwinski, B.; Szewczyk, M.; Smiley, E. J.; Winograd, N.; Garrison, B. J. *Anal. Chem.* **2003**, *75*, 4402−4407.

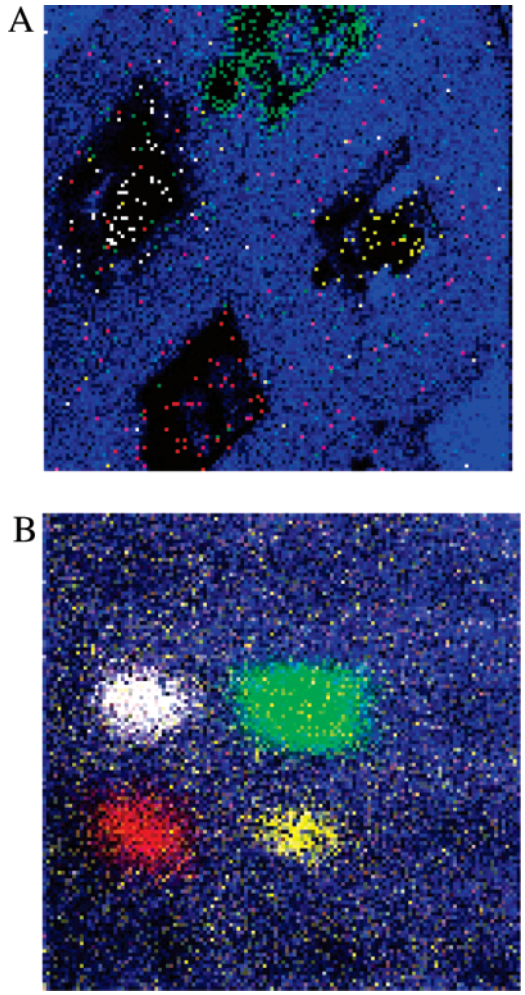

Figure 4. Positive ion SIMS images of phosphatidylglycerol (*m*/*z* 195, red), phosphatidylcholine (*m*/*z* 184, green), cholesterol (*m*/*z* 369, white), and sulfatide (*m*/*z* 264, yellow) delivered into silicon (*m*/*z* 28, blue) picoliter vials. 300 × 300 μm^2 field of view. (A) Image with an In^+ LMIS. (B) Image of the same picoliter vial array with a C_{60}^+ source. 1 × 1 mm^2 field of view.

over a liquid metal ion source is the ability to remove large, organic, molecular fragments from the surface.[29] Thus, the relative amounts of lipids sputtered with C_{60}^+ versus In^+ were comparatively much greater than the amount of atomic species sputtered.

The data reported in Figure 4A and B were collected on two different instruments. In a more thorough investigation of lipid signal enhancement, the secondary ion signals resulting from C_{60}^+ bombardment were compared to the signals resulting from Ga^+ bombardment on the same instrument. This eliminated variations in signal resulting from differences in instrument throughput and detector gain. The increased secondary ion signal from the selected lipids was remarkable, ranging from 40 to 1000 (Table 2, Figure 5). The high-mass peaks (above *m*/*z* 700) were enhanced the most with the cluster ion source, demonstrating the ability of C_{60}^+ bombardment to gently lift off intact molecules from the surface. We have generally observed two times the signal obtained with Ga^+ when using an In^+ primary projectile. The difference in yield between these two atomic projectiles probably stems from the difference in atomic weight. Thus, the signal enhancement when using a C_{60}^+ ion source versus In^+ ion source should be half as much but still highly significant, ranging from 20 to 500 improvement, which is consistent with the data in Figure 4.

Table 2. Comparison of the Secondary Ion Yields, Normalized to Primary Ion Current (nC), of Various Lipid Fragments as Obtained with a Ga^+ and a C_{60}^+ Primary Ion Source

lipid fragment	Ga^+ yield/nC	C_{60}^+ yield/nC	C_{60}/Ga
PC (*m*/*z* 86)	2.1×10^9	8.5×10^{11}	410
PC (*m*/*z* 184)	4.5×10^9	1.2×10^{12}	280
PC (*m*/*z* 224)	3.3×10^8	8.1×10^{10}	240
PC (*m*/*z* 734)	4.5×10^7	3.6×10^{10}	800
PE (*m*/*z* 124)	9.6×10^8	8.7×10^{10}	90
PE (*m*/*z* 142)	7.4×10^8	4.9×10^{10}	70
PE (*m*/*z* 691)	1.2×10^8	2.9×10^{10}	240
PE (*m*/*z* 122)	1.4×10^9	4.7×10^{11}	320
PE (*m*/*z* 140)	2.1×10^9	4.9×10^{11}	240
PG (*m*/*z* 195)	7.4×10^8	1.6×10^{11}	220
PG (*m*/*z* 767)	1.0×10^8	7.2×10^{10}	720
PI (*m*/*z* 241)	2.6×10^8	1.6×10^{11}	640
PI (*m*/*z* 259)	2.1×10^8	1.4×10^{11}	670
PI (*m*/*z* 299)	7.0×10^7	6.8×10^{10}	970
PS (*m*/*z* 208)	1.8×10^8	4.7×10^{10}	260
PS (*m*/*z* 757)	3.9×10^7	3.0×10^{10}	750
cholesterol (*m*/*z* 369)	2.3×10^8	1.6×10^{10}	70
cholesterol (*m*/*z* 385)	1.2×10^8	6.1×10^9	50
sulfatide (*m*/*z* 264)	5.0×10^8	2.2×10^{10}	40
sulfatide (*m*/*z* 906)	2.2×10^8	2.2×10^{11}	1000
silicon (*m*/*z* 28)	9.6×10^9	1.2×10^{11}	10

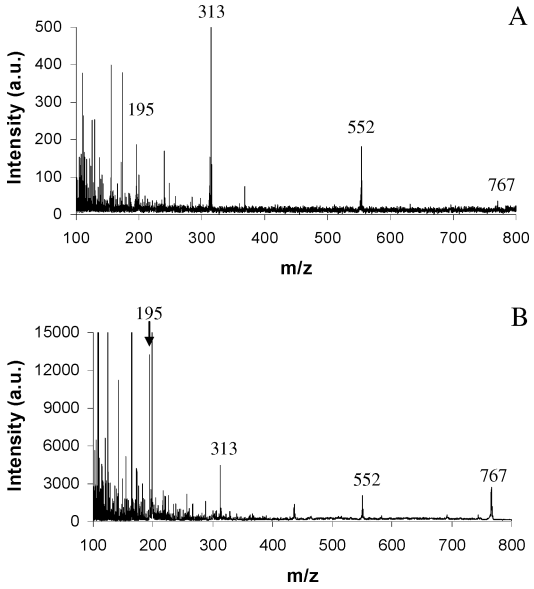

Figure 5. (A) + SIMS spectra of DPPG with a Ga^+ LMIS. (B) + SIMS spectra of DPPG with a C_{60}^+ source.

Identification of Lipids by SIMS in a Mixture. The absence of isobaric interferences between the different lipids of interest should allow them to be distinguished in a complex lipid mixture. As a rough mimic of the lipid complexity of a cell membrane, an equimolar mixture of seven lipids (PC, PE, PG, PS, PI, cholesterol, sulfatide) was examined with C_{60}^+ (Figure 6). Both positive ion (Figure 6A) and negative ion (Figure 6B) spectra were necessary to identify all seven lipids. PC was readily ionized and dominated the positive ion mixture spectrum. On the other hand, it was easily possible to identify the presence of PG, PS, PI, cholesterol, and sulfatide, demonstrating the ability of this technique for analyzing these lipids in complex mixtures. In contrast, the positive ions of PE did not give a strong signal, apparently for two reasons. First, there are many low-mass cholesterol fragments in the same mass range, thus masking the signal. Second, the *m*/*z* 124 and 142 peak areas are diminished by 5-fold when mixed with PC. The reason

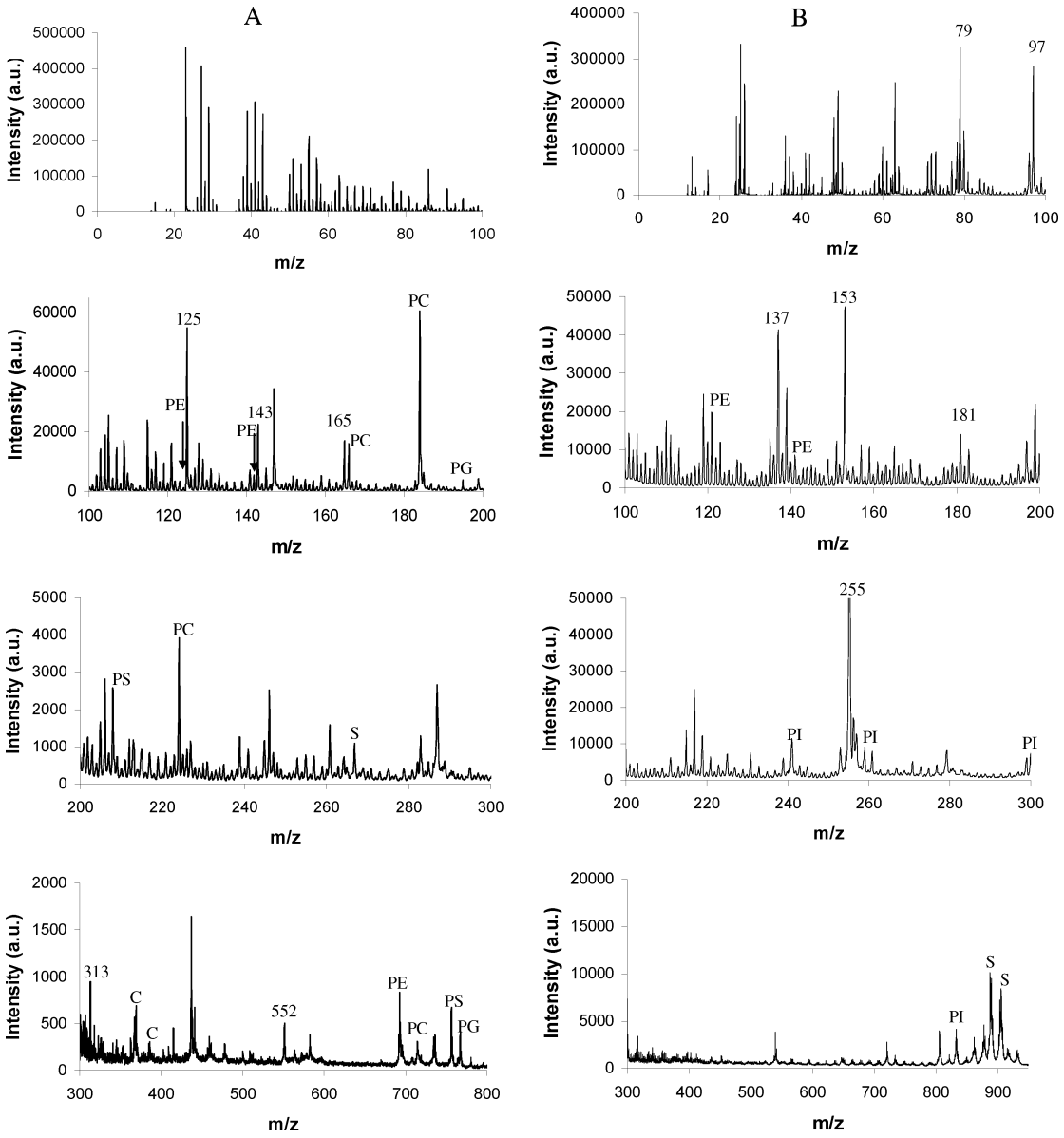

Figure 6. (A) + SIMS spectrum of an equimolar mixture of PC, PE, PG, PS, PI, cholesterol (C), and sulfatide (S) with a C_{60}^+ source. (B) − SIMS spectrum of the same mixture.

for the PE signal suppression by PC, observed in five separate experiments, probably arises from charge exchange processes within the matrix and is the subject of further investigation.

CONCLUSION

Using model systems and picoliter vials, we have shown that the signature peaks for phosphatidylcholine, phosphatidylglycerol, phosphatidylserine, phosphatidylinositol, cholesterol, and sulfatide in static SIMS can be used to distinguish several membrane lipids both spatially and in a mixture. The signature peaks were used to generate chemical maps of the lipids in a picoliter vial array and should be similarly valuable for molecular imaging the distribution of lipids on cell membranes. A 40−1000-fold improvement in signal from the lipids has been shown using a C_{60}^+ cluster ion source versus a Ga^+ ion source. The signal enhancement of lipids with cluster ion sources and SIMS is especially significant because it will allow for improved contrast between adjacent image pixels. Ultimately, this advancement in instrumentation will enable subtle differences in lipid concentration across a cell membrane to be probed.

ACKNOWLEDGMENT

The authors thank Dr. A. Daniel Jones for his assistance in mass spectral interpretation and for many helpful discussions. The authors also acknowledge the National Nanofabrication Facility (Cornell, NY) for use of their facilities in producing the picoliter vial arrays, particularly M. Rogosky for his assistance with the photolithographic process. Additionally, the authors are grateful for continued financial support from the NIH and additional instrumental funding from the NSF.

Received for review May 11, 2005. Accepted August 2, 2005.

AC0508189